Chemical Engineering Journal 149 (2009) 11–18

Contents lists available at ScienceDirect

Chemical Engineering Journal

journal homepage: www.elsevier.com/locate/cej

Valorization of coal fly ash by mechano-chemical activation Part I. Enhancing adsorption capacity

P. Stellacci [a,*], L. Liberti [a], M. Notarnicola [a], P.L. Bishop [b]

[a] Technical University of Bari, Department of Environmental Engineering & Sustainable Development, 74100 Taranto, I, Italy
[b] University of Cincinnati, Department Civil & Environmental Engineering, Cincinnati, OH 45221, USA

ARTICLE INFO

Article history:
Received 22 May 2007
Received in revised form 14 May 2008
Accepted 20 June 2008

Keywords:
Mechano-chemical activation
Coal fly ash
Activated carbon
Adsorption isotherms and kinetics
Phenol removal

ABSTRACT

The adsorption characteristics of coal fly ash have been enhanced by mechano-chemical activation with a high energy mono-planetary ball mill. The best performing sample for the adsorption of phenol from aqueous solution (i.e., fly ash with the higher carbon content and mechano-chemically activated for 4 h in N_2 atmosphere) was compared with powdered activated carbon, yielding quite encouraging results such as favorable adsorption isotherms, improved specific adsorption capacity and very fast adsorption rate. This provides new opportunities for utilizing fly ash in environmental protection applications like the stabilization/solidification treatment of hazardous waste and contaminated soil.

1. Introduction

Coal fly ash (FA), a finely divided powder resulting from carbon combustion (approximately 85 kg t^{-1} of coal), is an industrial waste expected to reach 800 Mt/year worldwide by the 2010, only a minor part of which (20–30%) is reused at present [1–3].

FA is basically made up of organic and inorganic coal combustion residues with trace hazardous contaminants such as polycyclic aromatic hydrocarbons, dioxins, heavy metals and even radioisotopes, depending on the carbon origin and combustion conditions. The organic fraction, consisting of unburned carbon and usually expressed by the loss on ignition (LOI), widely ranging from 2% to 90%, can potentially exhibit adsorption capacity, although it is usually almost negligible for practical applications [4–9]. The inorganic fraction, consisting of siliceous and/or aluminous material (artificial pozzolans), possesses some potential cementitious capacity. Both properties, if duly enhanced, can open new possibilities for using FA, thus turning a waste disposal problem into a cost-effective opportunity for reducing an environmental burden and opening new markets for FA.

Activated carbon, either in the powdered (PAC) or granular (GAC) form, typically exhibits a strong adsorption capacity for removing trace hazardous organics (and sometimes also inorganics) from civil and industrial effluents, but its cost often makes it unjustified for common pollution control applications [10–12]. Cheaper and more easily available adsorbents like low-grade natural products (coconut shell, lignite, natural wood, pillared clays, etc.) and even industrial by-products (blast furnace sludge, dust and slag from steel plants, carbon slurry waste from fertilizer plants, etc.) are accordingly being sought [13,14].

It has long been demonstrated that the mechano-chemical activation (MA) achieved with the so-called "high energy mills" (HEM) may greatly enhance the reactivity of solid particles [15,16]. MA has already found application in several fields, both at laboratory and industrial scales [17–22], including environmental protection [23–40].

A detailed investigation has been performed to evaluate the potential of MA for enhancing the adsorptive and pozzolanic properties of coal FA with the aim of using this latter as a potential substitute for PAC and Portland cement in the stabilization/solidification (S/S) treatment of contaminated soils [41]; the results obtained are illustrated as Part I and Part II of this presentation. Part I, in particular, describes how MA may enhance the adsorption capacity and the kinetics of FA towards phenol, a typical organic pollutant of industrial sites. Part II [42] illustrates the effective capacity of mechanically activated coal fly ash (MAFA) to

Abbreviations: AC, activated carbon; FA, fly ash; FA_x, fly ash with *x* LOI content; GAC, granular activated carbon; HEM, high energy mill; LOI, loss on ignition (%); MA, mechano-chemical activation; $MAFA_x$, mechano-chemically activated fly ash with *x* LOI content; PAC, powdered activated carbon; SEM, scanning electron microscopy; S/S, stabilization and solidification treatment.

* Corresponding author at: Viale del Turismo 8, 74100 Taranto, I, Italy.
Tel.: +39 099 4733203; fax: +39 099 4733203.
E-mail address: p.stellacci@poliba.it (P. Stellacci).

1385-8947/$ – see front matter © 2009 Published by Elsevier B.V.
doi:10.1016/j.cej.2008.06.043

Table 1
Average mineral analysis of the FA investigated and their eluate according to the EN 12457-2 leaching test

Mineral analysis		Eluate (pH 12.1)	
Compound	Concentration (w/w%)	Compound	Concentration ($mg\,l^{-1}$)
Silica (SiO_2)	43–81%	Al	3.0
		Ca	301
Alumina (Al_2O_3)	20–35%	Cd	<0.005
		Cr	0.15
Ferric oxide (Fe_2O_3)	5–15%	Cu	<0.005
		Fe	0.037
Calcium oxide (CaO)	1–5%	Mg	0.04
		Mn	<0.005
Potassium oxide (K_2O)	1.6–2%	Na	21
		Ni	<0.005
Titanium oxide (TiO_2)	1–2%	Pb	<0.01
		Zn	<0.01

prevent the leaching of phenol and Pb, a typical inorganic pollutant of industrial soils, if used during the S/S treatment of these.

2. Materials and methods

Coal fly ash samples with 27% and 80% LOI (i.e., FA_{27} and FA_{80}) and ≤300 μm maximum diameter were collected from the electrostatic precipitator of a large power plant (ENEL, Brindisi, S. Italy). Table 1 reports the average mineral analysis of such FA as well as of their eluate obtained after extraction in distilled water for 24 h at a $10\,l\,kg^{-1}$ liquid/solid ratio, according to the European Standard EN 12457-2 leaching test [43].

The Darco G-60 commercial PAC (J.T. Baker, Phillipsburg, NJ, USA), with a 100–325 U.S. mesh size (150–45 μm), was used for comparison purposes throughout the investigation.

The LOI and iodine number of both adsorbents were determined by the ASTM C311-00 [44] and D 4607-94 [45] methods, respectively. A Tristar 3000 porosimetry analyzer (Micromeritics, Norcross, GA, USA) was used to determine their surface areas according to the Brunauer, Emmett and Teller (BET) method as well as their porosity by N_2 adsorption at 77 K after 2 h purge at 150 °C using a Flow Prep 060 degassing unit (Micromeritics).

The surface morphology and the inorganic matter distribution of FA were investigated with a JEOL 850 Scanning Electron Microscope (Jeol Ltd., Tokyo, Japan) in conjunction with an Energy Dispersive Spectrometer (Tracor Northern, Middleton, WI, USA). X-ray diffractometers (XRD) spectra were obtained with a Philips X'Pert Pro PANanalytical (Almelo, The Netherlands) using mono-chromatized Cu Kα radiation at 40 kV and 50 mA at λ 1.54051 Å, a scanning speed of $4^\circ\ 2\theta\ min^{-1}$ and a step size of 0.1° in the range of 10–50° 2θ.

The mechano-chemically activated fly ash (MAFA) was obtained using a laboratory Pulverisette 6 mono-planetary high energy mill (Frisch, Idar-Oberstein, Germany); Figs. 1 and 2 show typical photography and a schematic representation, while Table 2 reports the technical characteristics for the operating conditions investigated. The HEM chamber was filled with 75 g of FA and 750 g of 5-mm diameter AISI 420C hardened-steel balls (12.5–14.5% Cr + 1% Ni), thus yielding a 10:1 ball to powder mass ratio, under inert N_2. Milling then started at a grinding speed of 400 rev min^{-1} and lasted up to 8 h, with 5 min stops every 15 min for heat dissipation.

Table 2
Technical characteristics of Fritsch Pulverisette 6 mono-planetary high energy mill

Parameter	Value
Vial radius (mm)	50
Vial depth (mm)	70
Vial net volume (ml)	550
Plate radius (mm)	60.8
Speed ratio ($r = \omega_v/\omega_p$)	−1.82

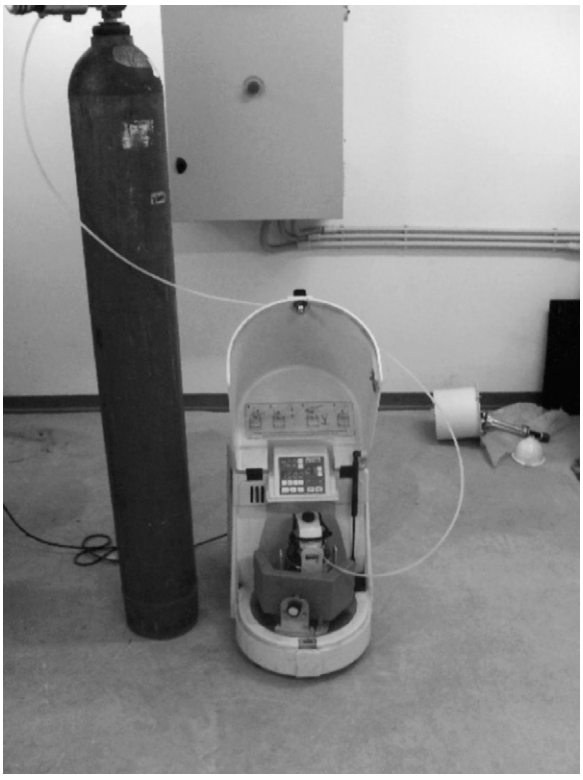

Fig. 1. Pulverisette 6 mono-planetary ball mill operating under N_2 atmosphere.

Size measurements with a Mod. 3600 Laser Particle Analyzer (Malvern Instruments, Worcestershire, UK) ensured that MAFA particles reached a diameter (≤63 μm) comparable with PAC.

XRD, BET and iodine number were checked after 1, 3, 4, 5 and 8 h in order to assess the structural modifications achieved with milling.

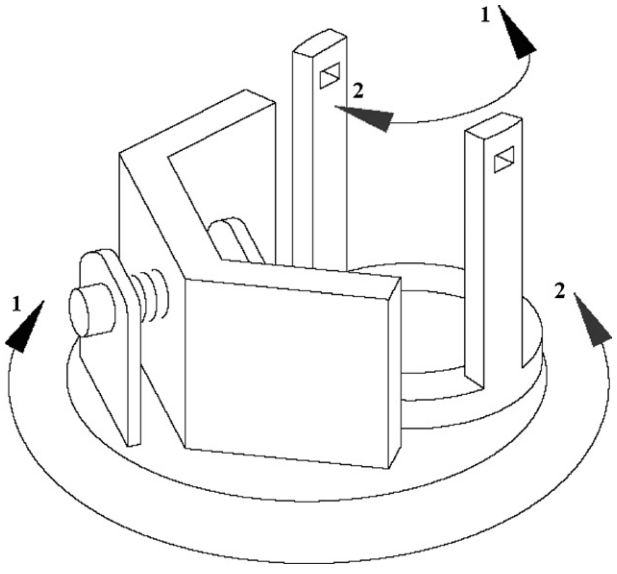

Fig. 2. Clockwise (1 → 2, vial) and anticlockwise (1 → 2, plate) rotation in planetary HE ball mill.

Table 3
Basic physical properties of the adsorbent materials investigated

Adsorbent	Iodine no. (mg g^{-1})	Specific surface area (m^2 g^{-1})	Volume of micropores (ml g^{-1})	U.S. mesh size	Particle size (μm)
PAC	881	938	0.344	100–325	150–45
FA_{27}	0	18	0.018		
FA_{80}	0	16	0.035	≥50	≤300
$MAFA_{27}$		54	0.125		
$MAFA_{80}$	238	69	0.180	≥230	≤63

PAC, Darco G-60 commercial powdered activated carbon; FA_{27}, fly ash with 27% LOI; FA_{80}, fly ash with 80% LOI; $MAFA_{27}$, fly ash with 27% LOI mechanically activated for 4 h; $MAFA_{80}$, fly ash with 80% LOI mechanically activated for 4 h.

The batch adsorption equilibrium experiments were carried out following the ASTM D 3860-98 bottle-point technique [46] using an aqueous solution of phenol, a typical highly soluble polar aromatic environmental contaminant. To that aim, a stock solution (20 g l^{-1}) of high-grade phenol (Sigma–Aldrich, 99.99%) was prepared and diluted with triply distilled deionized water to a concentration of 200 mg l^{-1}. 100 ml aliquots of this solution were placed in jacketed 250 ml Erlenmeyer flasks, thermostated at 25 or 40 °C to investigate the influence of temperature, and an increasing amount of the adsorbent material (0.03–0.3 g of PAC and 0.24–2.4 g of MAFA) was added to each flask. The solution was then stirred at 350 rpm with a Mod. AG.66 rotary agitator (Inlabo, Padua, I) for 2 h, a period adequate to reach almost complete equilibrium under the conditions investigated (see the adsorption rate tests). The pH of the solution at equilibrium had shifted to slightly acidic (≥6.0) and basic (≤9.0) in the flask containing added PAC or MAFA, respectively. This was presumably due to the leaching of acidic impurities from PAC, usually washed with acid before steam activation, and to solubilization of CaO present in FA (see Table 1). As phenol is a weak acid (pK_a 9.89 at 20 °C), it may be concluded that under these conditions undissociated phenol was the predominating species, with ≤10% phenate present at pH ≤ 9.0. It could be argued, however, that this latter poorly adsorbable anion should prevail during the S/S treatment due to the much higher pH (≥11) provided by the Portland cement [42].

After filtration through a 0.45-μm Iso-Disk filter (Supelco, San Francisco, CA, USA), residual phenol concentrations in solution were determined by measuring solution absorbance at 270 nm wavelength with a Lambda 25 UV/visible spectrophotometer (PerkinElmer, Wiesbaden, Germany), and the amount adsorbed was calculated by simple mass balance. Previous blank tests indicated a negligible release of organics adsorbing at that wavelength, which however was automatically accounted for by the data-handling software of the spectrophotometer.

Adsorption rate tests were carried out under similar conditions, with small samples of the suspension (5 ml) intermittently withdrawn for analysis during the 2 h duration of each test.

The experimental results were matched with model equations by a computerised non-linear optimization technique using the least-squares method.

All the experiments were carried out in duplicate, and the average values were used in further calculations.

3. Results and discussion

Table 3 shows the variation of the physical properties of the adsorbents investigated. From these data it appears that after MA, in agreement with the reduction of the maximum particle diameter, the specific surface of the FA with the larger carbon content (i.e., $MAFA_{80}$) almost quadrupled (from 16 to 69 m^2 g^{-1}, although still remaining much lower than the 938 m^2 g^{-1} of PAC while, not surprisingly, a still larger increase occurred in its micropore volume. This should reasonably yield a proportional enhancement of FA adsorption capacity.

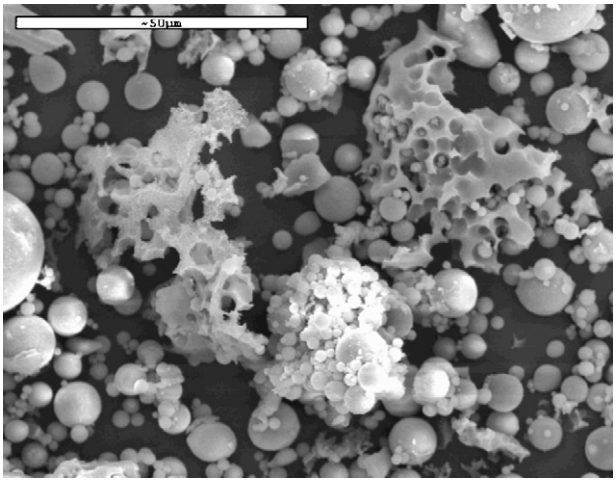

Fig. 3. SEM image of the coal fly ash investigated.

Fig. 3 shows a SEM image of the unburned carbonaceous portion of FA. Within the instrumental resolution range, the porous structure of the particle is clearly seen, with 1–10 μm macropores and embedded micro-sized glassy spheres (cenospheres), indicating that the unburned coal is a good candidate adsorbent.

The XRD patterns, shown in Fig. 4, indicate that the FA investigated had a negligible crystalline structure, with a major peak around 26°, and minor peaks around 16°, 32° and 34°, corresponding to quartz (SiO_2) and mullite ($3Al_2O_3{\cdot}2SiO_2$), respectively, and with the peak height obviously decreasing with its carbon content. As shown by the corresponding XRD in Fig. 5, such patterns disappear after 1 h milling, indicating the transformation of the crystalline phase into an amorphous one.

The specific surface of the FA varied in a non-linear fashion during the milling, as shown in Fig. 6, which indicates an optimum milling time for $MAFA_{80}$ around 4 h, when the increase of the exter-

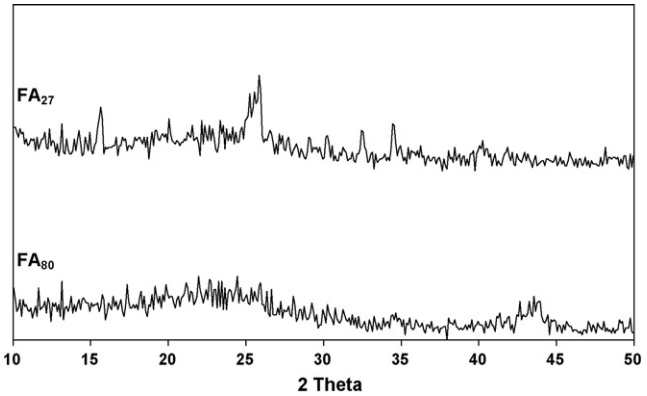

Fig. 4. X-ray diffraction patterns of the coal fly ash investigated.

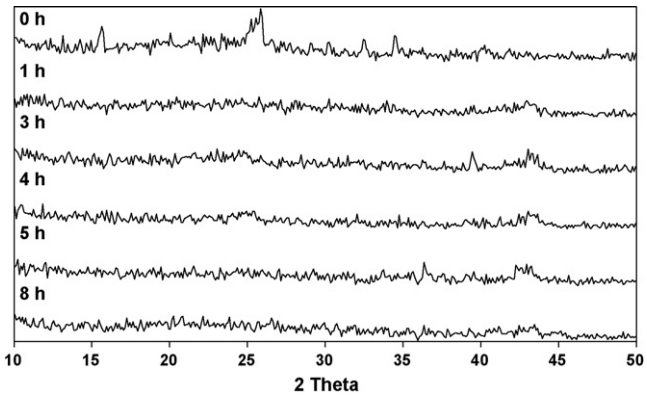

Fig. 5. X-ray diffraction patterns of $MAFA_{80}$ as a function of milling time.

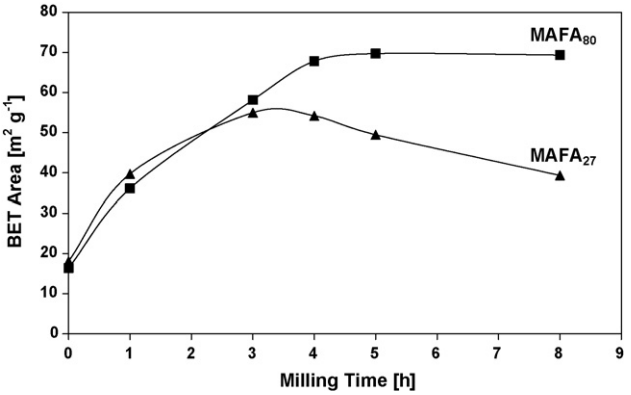

Fig. 6. Variation of the specific surface of FA as a function of milling time.

nal surface due to the further crushing of bigger crystals equals its decrease due to the secondary agglomeration of the powder already formed.

As most FA surfaces generally come from the regular pore networking, a change in its pore volume should parallel surface changes, as confirmed by Fig. 7.

Similar variations of the smaller pores, as indicated by the iodine number in Fig. 8, confirms that 4 h is the optimum milling time.

Accordingly, $MAFA_{80}$, i.e., coal fly ash with 80% LOI mechanochemically activated for 4 h under N_2 atmosphere, was considered the best performing specimen for the conditions investigated and hence was employed in further experiments.

Figs. 9 and 10 show the phenol adsorption isotherms at different temperatures for PAC and $MAFA_{80}$. Although PAC performed remarkably better, phenol adsorption by $MAFA_{80}$ cannot be disregarded. In fact, accounting for their specific surfaces, this latter yields a much greater specific adsorption capacity (203 μg phenol m^{-2} *vs.*129 μg phenol m^{-2}), in agreement with the multi- (Freundlich) and mono- (Langmuir) layer adsorption mechanisms postulated for $MAFA_{80}$ and PAC, respectively (see later).

Phenol adsorption by MAFA can be attributed to its morphology, where a smaller interstitial free surface area is available for aggregation of the adsorbate molecules due to the high temperature of coal combustion and fly ash formation. As previously seen, the MAFA particles have lower percentages of micro- or macrop-

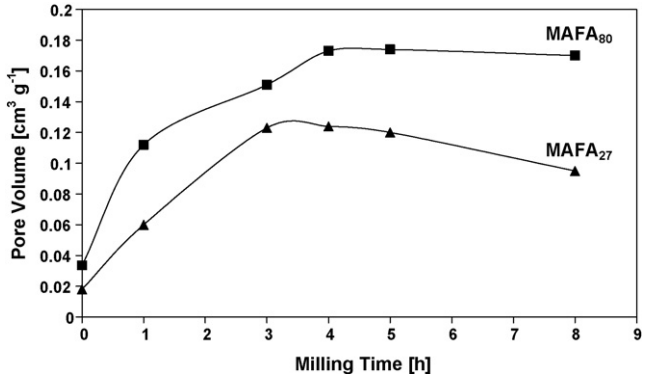

Fig. 7. Variation of the pore volume of FA as a function of milling time.

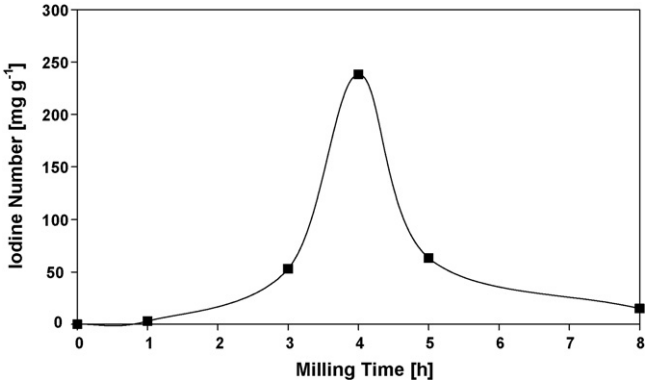

Fig. 8. Variation of the I_2 number of FA as a function of milling time ($MAFA_{80}$).

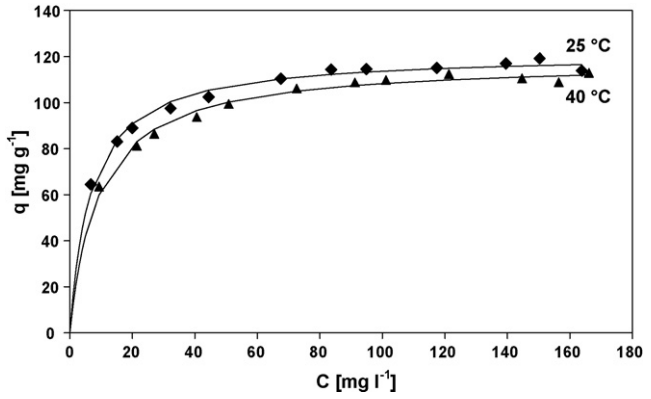

Fig. 9. Phenol adsorption isotherms by PAC (solid lines according to Langmuir model by Eq. (1); initial phenol concentration 200 mg l^{-1}; adsorbent mass 0.3–3 g l^{-1}).

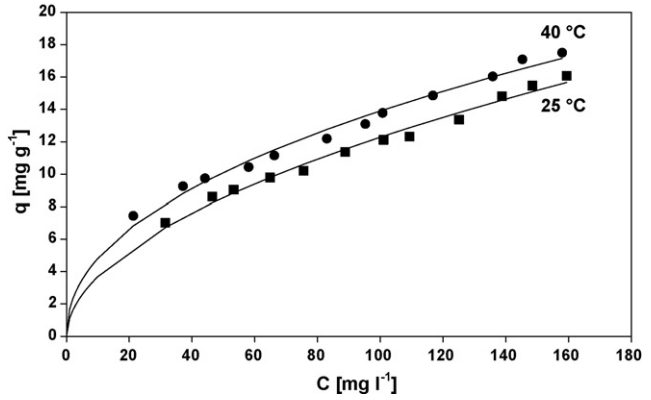

Fig. 10. Phenol adsorption isotherms by $MAFA_{80}$ (solid lines according to Freundlich model by Eq. (5); initial phenol concentration 200 mg l^{-1}; adsorbent mass 2.4–24 g l^{-1}).

Table 4
Experimental isotherm parameters for Phenol adsorption

Adsorbent	T (°C)	Langmuir			Freundlich		
		X_m (mg g^{-1})	K_L	R^2	K_F (mol g^{-1} (l mol)$^{1/n}$)	$1/n$	R^2
PAC	25	121.28	1,49,408.16	0.9811	54.15	0.1593	0.9288
	40	118.04	1,10,627.89	0.9815	48.59	0.1710	0.9249
$MAFA_{80}$	25	24.36	10,598.38	0.9590	1.1093	0.5221	0.9850
	40	23.39	15,501.80	0.9389	1.6699	0.4602	0.9833

ores than PAC (238 *vs*. 881 I_2 Number, see Table 3), so their smaller surface results in a lower absolute, but a larger specific, adsorption capacity.

From a practical point of view, the higher amount of $MAFA_{80}$ required to achieve adsorption results comparable with PAC may still be cost-effective in large scale applications; this needs to be evaluated on a case by case basis.

From a theoretical point of view, the different performances of the two adsorbents towards phenol deserve comment.

3.1. Equilibrium modeling

3.1.1. PAC (Fig. 9)

(a) The temperature had an unfavorable effect on the adsorption capacity, as expected due to the usually exothermic nature of the adsorption process.
(b) The shape of the isotherms, typically corresponding to a type I [47] and L-shaped [48] isotherm, is peculiar to the Langmuir model. This latter reportedly occurs when the adsorption is restricted to a mono-layer on the surface, where a finite number of identical sites are homogeneously distributed [49], as described by the equation:

$$\frac{q}{X_m} = \frac{K_L(C/C^{\vartheta})}{1 + K_L(C/C^{\vartheta})} \quad (1)$$

where q is the amount of phenol adsorbed per unit mass of carbon at equilibrium (mg g^{-1}); X_m is the maximum amount of phenol adsorbed per unit mass of carbon at equilibrium (mg g^{-1}); K_L is the equilibrium constant (dimensionless), C is the equilibrium concentration of phenol in solution (mg l^{-1}); C^{ϑ} is the equilibrium concentration of water in solution (10^6 mg l^{-1}).

K_L and X_m values can be easily obtained by the intercept $1/X_m$ and the slope $1/(X_m K_L)$ by plotting Eq. (1), indicating an unfavorable, linear, favorable or irreversible isotherm for K_L <0, =0, >0 or =+∞, respectively.

Variation of the equilibrium constant K_L with the temperature allows one to calculate the Gibbs free energy (ΔG^{ϑ}), enthalpy (ΔH^{ϑ}) and entropy (ΔS^{ϑ}) variation according to the known equations

$$\Delta G^{\vartheta} = \Delta H^{\vartheta} - T\Delta S^{\vartheta} = -RT \ln K_L \,(\mathrm{J\,mol^{-1}}) \quad (2)$$

$$\Delta H^{\vartheta} = R\frac{T_1 T_2}{T_2 - T_1} \ln \frac{K_{L2}}{K_{L1}} \,(\mathrm{J\,mol^{-1}}) \quad (3)$$

$$\Delta S^{\vartheta} = \frac{\Delta H^{\vartheta} - \Delta G^{\vartheta}}{T} \,(\mathrm{J\,mol^{-1}\,K^{-1}}) \quad (4)$$

3.1.2. $MAFA_{80}$ (Fig. 10)

(a) The adsorption of phenol was shown to be endothermic, increasing with temperature. This typically occurs when the solute is less strongly adsorbed than the accompanying solvent, and adsorption results from the competing mechanisms of desorption of solvent (water) and adsorption of solute [50]. Phenol has to displace more than one water molecule and this causes endothermicity.
(b) The shape of the isotherms, typically corresponding to a type III [47] and the H-shaped [48] isotherm, is peculiar to the Freundlich empirical model, valid for multilayer adsorption, as represented by the equation:

$$q = K_F C^{1/n} \quad (5)$$

K_F (first equilibrium constant [mol g^{-1} (l mol)$^{1/n}$]) and n (second equilibrium constant [dimensionless]) may be easily obtained by linear regression of the experimental data through a log–log plot of Eq. (5). The $1/n$ exponent dictates the shape of the isotherm, indicating an unfavorable, linear, favorable or irreversible isotherm if >1, =1, 0 < $1/n$ < 1 or =0, respectively.

The experimental values of the adsorption parameters for both models and adsorbents at the temperatures investigated are reported in Table 4. As confirmed by the standard non-linear regression analysis, the Langmuir and Freundlich equations represented the best-fit model for phenol adsorption onto PAC and $MAFA_{80}$, respectively. The predicted maximum uptake X_m value for PAC falls within the expected range [51].

According to the Langmuir and Freundlich model, the values of $K_L > 0$ and $0 < 1/n < 1$, respectively, indicate that, for the conditions investigated, phenol adsorption occurs favorably with both adsorbents.

As shown in Table 5, the negative values of ΔG^{ϑ} confirm the spontaneous nature of phenol adsorption onto both adsorbents.

The negative and positive values of ΔH^{ϑ} confirm the exothermic and endothermic nature of phenol adsorption onto PAC and $MAFA_{80}$, respectively, whereas the low absolute ΔH^{ϑ} values tend to rule out *chemisorption*, as discussed later.

The positive entropy change ΔS^{ϑ} for both adsorbents, finally, indicates an increasing mobility at the carbon-solution interface during the adsorption process.

3.2. Kinetics modeling

Figs. 11 and 12 show the kinetics of phenol adsorption in different operating conditions. From these results the following considerations may be drawn:

(a) The average uptake rate of PAC (≈10 mg phenol min^{-1} g^{-1} in Fig. 11) is ≈10-fold higher than $MAFA_{80}$ (≈1 mg phenol min^{-1} g^{-1} in Fig. 12). However, if one considers

Table 5
Experimental thermodynamic parameters for phenol adsorption between 25 and 40 °C

Adsorbent	ΔG^{ϑ} (kJ mol^{-1})	ΔH^{ϑ} (kJ mol^{-1})	ΔS^{ϑ} (kJ mol^{-1} K^{-1})
PAC	−29.519	−15.536	0.047
$MAFA_{80}$	−22.963	19.659	0.143

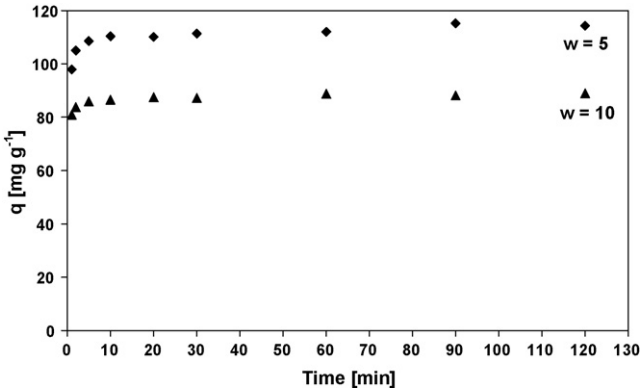

Fig. 11. Phenol adsorption rate by PAC at 25 °C (initial phenol concentration 200 mg l^{-1}; $w = g_{adsorbent}\ g_{solute}^{-1}$).

that PAC has a ≈14-fold larger specific surface, then $MAFA_{80}$ exhibits a faster surface uptake rate (14 μg phenol min^{-1} m^{-2} *vs.* 10 μg phenol min^{-1} m^{-2}), in agreement with the multi- (Freundlich) *vs.* mono- (Langmuir) layer adsorption mechanism assumed for the two adsorbents, respectively.

(b) Both adsorbents show very fast adsorption rates, with saturation reached in ≤5 min.

(c) If one compares the above kinetics in terms of fractional attainment of equilibrium U

$$U = \frac{q}{q_\infty} \times 100 \tag{6}$$

where q and q_∞ are the amounts of phenol (mg g^{-1}) adsorbed at time t (min) and at equilibrium, respectively, as shown in Fig. 13, both adsorbents exhibit substantially similar adsorption rates, irrespective of their nature and the adsorbent to solute ratio (w).

The explanation of these results is not straightforward. It has long been stated [10,52] that the adsorption of chemicals from solution by activated carbon occurs essentially through three consecutive steps, the slowest of which (if any) represents the rate-limiting step: *film diffusion* (transport of the adsorbate through a stagnant liquid film surrounding the adsorbent exterior surface), *particle diffusion* (transport of the adsorbate within the pores of the adsorbent) and *chemi-* or *physi-sorption* (the adsorption process itself, wherein the adsorbate is bound to the active site along the adsorbent interior surface by chemical reaction or by physical interaction).

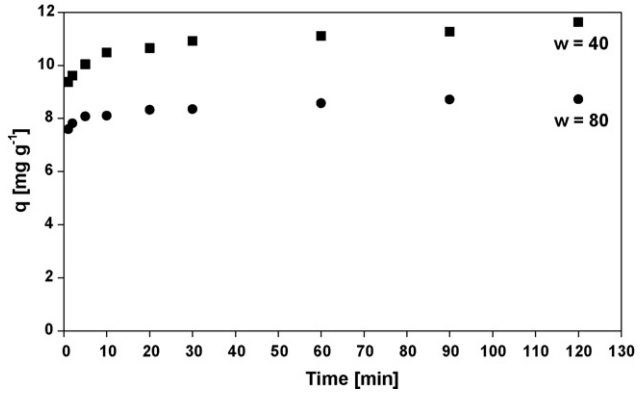

Fig. 12. Phenol adsorption rate by $MAFA_{80}$ at 25 °C (initial phenol concentration 200 mg l^{-1}; $w = g_{adsorbent}\ g_{solute}^{-1}$).

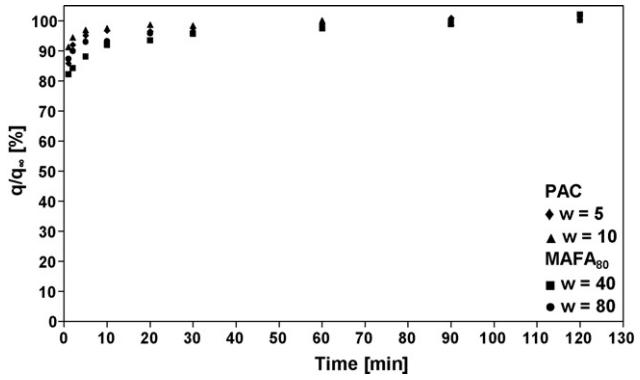

Fig. 13. Kinetics of phenol adsorption expressed as fractional attainment of equilibrium (initial phenol concentration 200 mg l^{-1}; $w = g_{adsorbent}\ g_{solute}^{-1}$).

The diffusion-controlled processes (either *film* or *particle*) are usually slow. They are described by various mathematical developments of the well-known Fick' and Nernst–Planck' equations, which depend on the diffusion coefficient of the adsorbate (for phenol as low as $\leq 10^{-5}$ and $\leq 10^{-7}$ cm^2 s^{-1} in the liquid and in the particle phases, respectively [53]).

For a given adsorbent–adsorbate system, the predominance of the *diffusion* (either *film* or *particle*) or the *chemi/physi-sorption* control may vary with the operating conditions: good solution stirring and/or extremely small particle diameters, as achieved in the present "completely mixed batch reactor" experiments with finely powdered adsorbents, tend to minimize film and particle diffusion control, respectively.

The very fast phenol adsorption rate, together with the value of the thermodynamic functions exhibited by both adsorbents in the present investigation, indicates that:

1. diffusion control may be ruled out, due to the thin thickness of the liquid film that surrounds each adsorbent particle and to the extremely small diameter of this latter;
2. chemisorption control may also be excluded, due to the low absolute value of ΔH^θ;
3. the process can then be classified as *physi-sorption*, occurring essentially at the external surface of each adsorbent particle.

Accordingly, the present experimental data have been matched by regression analysis with the well-known rate equations for physi-sorption [54]:

$$\ln\left(1 - \frac{q}{q_\infty}\right) = -k_1 t \quad \text{(pseudo-first-order kinetics)} \tag{7}$$

where k_1, the pseudo-first-order equilibrium rate constant (min^{-1}), may be obtained from the slope of the plot, and/or

$$\frac{t}{q} = \frac{1}{k_2 q_\infty^2} + \frac{t}{q_\infty} \quad \text{(second-order kinetics)} \tag{8}$$

where q_∞ and k_2, the pseudo-second-order equilibrium rate constant (g mg^{-1} min^{-1}), may be obtained from the slope and intercept of the plot, respectively.

As shown by Figs. 14 and 15 as well as by the kinetic parameters obtained by regression analysis reported in Table 6, the second-order physi-sorption kinetics appear to better fit the present experimental data for both adsorbents, as indicated by the higher correlation coefficients and by the calculated q_∞ values, closer to the experimental ones.

This finding agrees with the results achieved in similar rate studies [19,55–57].

Table 6
Experimental kinetic parameters for phenol adsorption at 25 °C

Adsorbent	w	q^*_∞ (mg g^{-1})	First-order rate			Second-order rate		
			q_∞ (mg g^{-1})	k_1 (min^{-1})	R^2	q_∞ (mg g^{-1})	k_2 (g mg^{-1} min^{-1})	R^2
PAC	5	114.12	111.25	2.0424	0.7520	114.94	0.0176	0.9999
	10	88.68	87.25	2.5572	0.6824	89.29	0.0448	1.0000
$MAFA_{80}$	40	11.39	10. 78	1.8495	0.4412	11.56	0.0777	0.9994
	80	8.68	8.35	2.2721	0.4649	8.74	0.1715	0.9999

q^*_∞ = experimental value; q_∞ = calculated value.

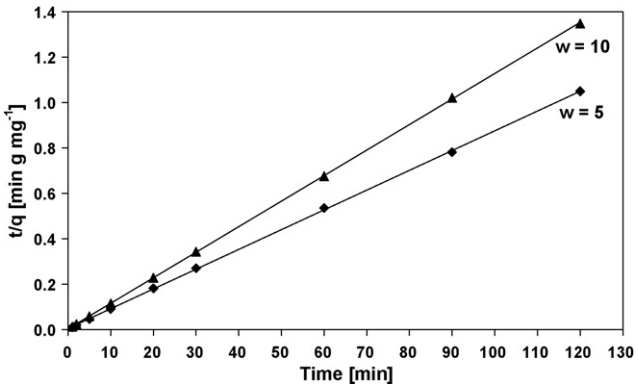

Fig. 14. Kinetics of phenol removal by PAC at 25 °C (solid lines according to second-order model by Eq. (7); initial phenol concentration 200 mg l^{-1}).

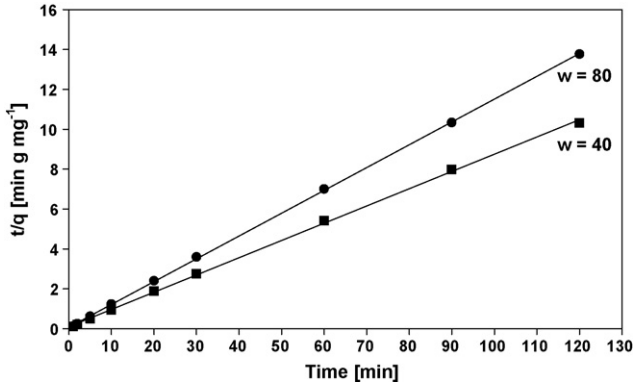

Fig. 15. Kinetics of phenol removal by $MAFA_{80}$ at 25 °C (solid lines according to second-order model by Eq. (7); initial phenol concentration 200 mg l^{-1}).

4. Conclusions

The results of the experimental investigation on the potential of mechano-chemical activation to enhance the adsorption capacity of coal fly ash offered the following indications:

(a) under the operating conditions investigated, the mechano-chemically activation of coal fly ash with the largest LOI ($MAFA_{80}$) induced a remarkable increase of its surface area and microporosity (although still remaining much lower than PAC);
(b) accordingly, $MAFA_{80}$ developed an appreciable potential for the adsorption of phenol, a typical organic pollutant of industrial emissions and contaminated soils;
(c) both PAC and $MAFA_{80}$ adsorbents showed favorable adsorption equilibrium towards phenol ($\Delta G^\vartheta < 0$ and $\Delta S^\vartheta > 0$, particularly for $MAFA_{80}$);
(d) contrary to the exothermic Langmuir-type mono-layer adsorption mechanism exhibited by PAC, $MAFA_{80}$ showed an endothermic Freundlich-type multi-layer adsorption mechanism yielding a higher surface adsorption capacity (mg adsorbate/m^2 adsorbent);
(e) thanks to the micron-size achieved through mechano-chemical activation, $MAFA_{80}$ also exhibited an unexpectedly fast phenol adsorption rate, following a physi-sorption-controlled second-order kinetics.

Accounting for its very low cost and wide availability, it may be concluded that coal fly ash properly activated by mechano-chemical treatment could offer a valid alternative to activated carbon for environmental applications. To this aim, MAFA behaviour as a potential substitute for PAC and Portland cement during S/S treatment of contaminated soil has been evaluated and described in Part II of this study [42].

Acknowledgments

The authors would like to thank Mr. Alberto Stella, Covecom SpA (Milan, I) for the financial support and Prof. Federico Cangialosi, Technical University of Bari, I, for useful comments and suggestions during this the investigation.

References

[1] P.F. Sens, Flue Gas and Fly Ash, Routledge, 1990.
[2] R.C. Joshi, Fly Ash in Concrete: Production, Properties and Uses, Taylor & Francis, 1997.
[3] L.K.A. Sear, The Properties and Use of Coal Fly Ash: A Valuable Industrial By-Product, Thomas Telford Editor, 2006.
[4] S. Ram Mohan Rao, V.V. Basava Rao, Removal of hexavalent chromium from electroplating industrial effluents by using hydrothermally treated fly ash, J. Appl. Sci. 7 (2007) 2088–2092.
[5] C.D. Woolard, J. Strong, C.R. Erasmus, Evaluation of the use of modified coal ash as a potential sorbent for organic waste streams, Appl. Geochem. 17 (2002) 1159–1164.
[6] S. Wang, M. Soudi, L. Li, Z.H. Zhu, Coal ash conversion into effective adsorbents for removal of heavy metals and dyes from wastewater, J. Hazard. Mater. B 133 (2006) 243–251.
[7] C.D. Woolard, K. Petrus, M. van der Horst, The use of a modified fly ash as an adsorbent for lead, Water SA 26 (2000) 531–536.
[8] P.J. Pretoriusa, C.D. Woolard, The surface chemical properties of novel high surface area solids synthesized from coal fly ash, S. Afr. J. Chem. 56 (2003) 34–39.
[9] S.S. Choi, J.C. Chung, S.H. Yeom, Removal of phosphate using coal fly ash from a thermal power station, J. Ind. Eng. Chem. 11 (2005) 638–642.
[10] J. Toth, Adsorption: Theory, Modeling and Analysis, Marcel Dekker Editor, 2002.
[11] V. Amicarelli, G. Baldassarre, L. Liberti, Investigation of low-temperature regeneration of activated carbon, J. Therm. Anal. Calorim. 18 (1980) 155–160.
[12] M. Streat, J.W. Patrick, M.J. Camporro Perez, Sorption of phenol and *para*-chlorophenol from water using conventional and novel activated carbons, Water Res. 29 (1995) 467–472.
[13] Z. Aksu, J. Yener, A comparative adsorption/biosorption study of mono-chlorinated phenols onto various sorbents, Waste Manage. 21 (2001) 695–702.
[14] G. Dursun, H. Çiçek, A.Y. Dursun, Adsorption of phenol from aqueous solution by using carbonised beet pulp, J. Hazard. Mater. B125 (2005) 175–182.
[15] W. Ostwald, Handbuch der allgemeinen chemie, Leipzig, 1919.
[16] V.V. Boldyrev, Experimental methods in the mechanochemistry of inorganic solids, in: H. Herman (Ed.), Treatise on Materials Science and Technology, vol. 19, Academic Press, 1983.
[17] N.J. Welham, J.S. Williams, Extended milling of graphite and activated carbon, Carbon 36 (1998) 1309–1315.

[18] V.V. Molchanov, R.A. Buyanov, Scientific grounds for the application of mechanochemistry to catalyst preparation, Kinet. Catal. 42 (2001) 366–374.
[19] N.J. Welham, V. Berbenni, P.G. Chapman, Increased chemisorption onto activated carbon after ball milling, Carbon 40 (2002) 2307–2315.
[20] K.G. Korolev, O.I. Lomovsky, O.A. Rozhanskaya, V.G. Vasil'ev, Mechano-chemical preparation of water-soluble forms of triterpene acids, Chem. Nat. Compd. 39 (2003) 366–377.
[21] V.V. Zyryanov, Ultrafast mechanochemical synthesis of mixed oxides, Inorg. Mater. 41 (2005) 378–392.
[22] H. Onoda, D. Mori, K. Kojima, H. Nariai, Mechanochemical effects on the formation and properties of various nickel phosphates, Inorg. Mater. 41 (2005) 1089–1096.
[23] A.K. Hall, J.M. Harrowfield, R.J. Hart, P.G. McCormick, Mechanochemical reaction of DDT with calcium oxide, Environ. Sci. Technol. 30 (1996) 3401–3407.
[24] S. Saeki, J. Kano, F. Saito, K. Shimme, S. Masuda, T. Inoue, Effect of additives on dechlorination of PVC by mechanochemical treatment, J. Mater. Cycles Waste Manage. 3 (2001) 20–23.
[25] N.J. Welham, Mechanochemical processing of gold-bearing sulphides, Miner. Eng. 14 (2001) 341–347.
[26] H. Mio, S. Saeki, J. Kano, F. Saito, Estimation of mechanochemical dechloration rate of poly(vinyl chloride), Environ. Sci. Technol. 36 (2002) 1344–1348.
[27] F. Cavalieri, F. Padella, Development of composite materials by mechano-chemical treatment of post-consumer plastic waste, Waste Manage. 22 (2002) 913–916.
[28] K.G. Korolev, A.I. Golovanova, N.N. Maltseva, O.I. Lomovski, V.L. Salenko, V.V. Boldyrev, Application of mechanical activation to decomposition of toxic chlorinated organic compounds, Chem. Sustain. Develop. 11 (2003) 489–496.
[29] P. Plescia, D. Gizzi, S. Benedetti, L. Camillucci, C. Fanizza, P. De Simone, F. Pagletti, Mechanochemical treatment to recycling asbestos-containing waste, Waste Manage. 23 (2003) 209–218.
[30] S. Saeki, J. Lee, Q. Zhang, F. Saito, Co-grinding $LiCoO_2$ with PVC and water leaching of metal chlorides formed in ground product, Int. J. Miner. Process. 74S (2004) S373–S378.
[31] M.D.R. Pizzigallo, A. Napola, M. Spagnuolo, P. Ruggiero, Mechanochemical removal of organo-chlorinated compounds by inorganic components of soil, Chemosphere 55 (2004) 1485–1492.
[32] J. Ryou, Improvement on reactivity of cementitious waste materials by mechano-chemical activation, Mater. Lett. 58 (2004) 903–906.
[33] V. Birke, J. Mattik, D. Runne, Mechanochemical reductive dehalogenation of hazardous polyhalogenated contaminants, J. Mater. Sci. 39 (2004) 5111–5116.
[34] K. Miyoshi, T. Nishio, A. Yasuhara, M. Morita, T. Shibamoto, Detoxification of hexachlorobenzene by dechlorination with potassium–sodium alloy, Chemosphere 55 (2004) 1439–1446.
[35] G. Intini, L. Liberti, M. Notarnicola, T. Pastore, Mechanochemical treatment for remediation of harbour sediments contaminated by PCBs and PAHs, in: R.F. Olfenbuttel, P.J. White (Eds.), Remediation of Contaminated Sediments. Finding Achievable Risk Reduction Solutions, Battelle Press, Columbus, OH, 2005, ISBN 1-57477-150-F, CD-ROM.
[36] V.V. Boldyrev, N.Z. Lyakhov, in: Proceedings of the V International Conference on Mechano-chemistry and Mechanical Alloying "Income 2006", Novosibirsk, Russia, 2006. http://www.solid.nsc.ru/INCOME2006.
[37] F. Cangialosi, G. Intini, L. Liberti, M. Notarnicola, T. Pastore, S. Sasso, Investigation on degradation of PAHs by mechanochemical treatment, in: Proceedings of the V International Conference on Mechanochemistry and Mechanical Alloying "Income 2006", Novosibirsk, Russia, 2006. http://www.solid.nsc.ru/INCOME2006.
[38] V.A. Drebushchak, G. Intini, L. Liberti, M. Notarnicola, T. Pastore, T.N. Drebushchak, V.V. Boldyrev, Dechlorination of contaminated sediments of Ionian sea: thermo-analytical investigation, J. Therm. Anal. Calorim. 90 (2007) 143–146.
[39] F. Cangialosi, G. Intini, L. Liberti, D. Lupo, M. Notarnicola, T. Pastore, Mechanochemical treatment of contaminated marine sediments. Part I. PCBs degradation, Chem. Sustain. Develop. 15 (2007) 147–156.
[40] F. Cangialosi, G. Intini, L. Liberti, M. Notarnicola, T. Pastore, S. Sasso, Mechanochemical treatment of contaminated marine sediments. Part II. PAHs degradation, Chem. Sustain. Develop. 15 (2007) 139–145.
[41] P. Stellacci, Valorization of coal fly ash in stabilization/solidification of contaminated soil, Ph.D. Thesis, Technical University of Bari, I, 2007.
[42] P. Stellacci, L. Liberti, M. Notarnicola, P.L. Bishop, Valorisation of coal fly ash by mechano-chemical activation. Part II. Enhancing pozzolanic reactivity, Chem. Eng. J., submitted for publication.
[43] EN 12457-2, Characterisation of waste. Leaching—Compliance test for leaching of granular waste material and sludges. Part 2: One stage batch test at a liquid to solid ratio of 10 l kg^{-1} for materials with particle size below 4 mm (without or with size reduction), 2004.
[44] ASTM C311-00, Standard test methods for sampling and testing fly ash or natural pozzolans for use as a mineral admixture in Portland-cement concrete, American Society for Testing and Materials, West Conshohocken, PA, 2000.
[45] ASTM D 4607-94, Standard test method for determination of iodine number of activated carbon, American Society for Testing and Materials, West Conshohocken, PA, 1994.
[46] ASTM D 3860-98, Standard practice for determination of adsorptive capacity of activated carbon by aqueous phase isotherm technique, American Society for Testing and Materials, West Conshohocken, PA, 2003.
[47] K.S.W. Sing, D.H. Everett, R.A.W. Haul, L. Moscou, R.A. Pietotti, J. Rouquerol, T. Siemienieska, Reporting physisorption data for gas/solid systems with special reference to the determination of surface area and porosity, Pure Appl. Chem. 57 (1985) 603–619.
[48] C.H. Giles, T.H. McEwan, S.N. Nakhwa, D. Smith, Studies in adsorption. Part XI. A system of classification of solution adsorption isotherms and its use in diagnosis of adsorption mechanism and in measurement of specific surface areas of solids, J. Chem. Soc. (1960) 3973–3993.
[49] D.F. Evans, H. Wennerstrom, The Colloidal Domain: Where Physics, Chemistry, Biology, and Technology Meet, 2nd ed., Wiley–VCH, 1999.
[50] V.C. Srivastava, M.M. Swamy, I.D. Mall, B. Prasad, I.M. Mishra, Adsorptive removal of phenol by bagasse fly ash and activated carbon: equilibrium, kinetics and thermodynamics, Colloids Surf. A 272 (2006) 89–104.
[51] B. Okolo, C. Park, M.A. Keane, Interaction of phenol and chlorophenols with activated carbon and synthetic zeolites in aqueous media, J. Colloid Interface Sci. 226 (2000) 308–317.
[52] J.W. Weber, Physicochemical Processes for Water Quality Control, Wiley-Interscience, New York, NY, 1972.
[53] D.R. Lide, Handbook of Chemistry and Physics, CRC Press, Cleveland, OH, 2004.
[54] S. Lagergren, Zur theorie der sogenannten adsorption gelöster stoffe, Kungliga Svenska Vetenskapsakademiens, Handlingar 24 (1898) 1–39.
[55] K. Mohanty, D. Das, M.N. Biswas, Adsorption of phenol from aqueous solutions using activated carbons prepared from Tectona Grandis sawdust by $ZnCl_2$ activation, Chem. Eng. J. 115 (2005) 121–131.
[56] V.V. Goud, K. Mohanty, M.S. Rao, N.S. Jayakumar, Phenol removal from aqueous solutions using tamarind nut shell activated carbon: batch and column study, Chem. Eng. Technol. 28 (2005) 814–821.
[57] G. Dursun, H. Cicek, A. Dursun, Adsorption of phenol from aqueous solution by using carbonised beet pulp, J. Hazard. Mater. B 125 (2005) 175–182.